TOXICOLOGICAL SCIENCES **123(2)**, 550–562 (2011)
doi:10.1093/toxsci/kfr191
Advance Access publication July 21, 2011

Multi-species Analyses of Direct Activators of the Constitutive Androstane Receptor

Curtis J. Omiecinski,*[,1] Denise M. Coslo,* Tao Chen,* Elizabeth M. Laurenzana,* and Richard C. Peffer†

*Center for Molecular Toxicology and Carcinogenesis, Department of Veterinary and Biomedical Sciences, Penn State University, University Park, Pennsylvania 16802; and †Syngenta Crop Protection, LLC., Greensboro, North Carolina, 27419-8300

[1]To whom correspondence should be addressed at Penn State University, 101 Life Sciences Building, University Park, PA 16802. Fax: (814) 863-1696. E-mail: cjo10@psu.edu.

Received May 20, 2011; accepted July 11, 2011

The constitutive androstane receptor (CAR; NR1I3) is a member of the nuclear receptor superfamily and functions as an important xenochemical sensor and transcriptional modulator in mammalian cells. Upon chemical activation, CAR undergoes nuclear translocation and heterodimerization with the retinoid X receptor subsequent to its DNA target interaction. CAR is unusual among nuclear receptors in that it possesses a high level of constitutive activity in cell-based assays, obscuring the detection of ligand activators. However, a human splice variant of CAR, termed CAR3, exhibits negligible constitutive activity. In addition, CAR3 is activated by ligands with similar specificity as the reference form of the receptor. In this study, we hypothesized that similar CAR3 receptors could be constructed across various mammalian species' forms of CAR that would preserve species-specific ligand responses, thus enabling a more sensitive and differential screening assessment of CAR response among animal models. A battery of CAR3 receptors was produced in mouse, rat, and dog and comparatively evaluated with selected ligands together with human CAR1 and CAR3 in mammalian cell reporter assays. The results demonstrate that the 5-amino acid insertion that typifies human CAR3 also imparts ligand-activated receptor function in other species' CAR while maintaining signature responses in each species to select CAR ligands. These variant constructs permit *in vitro* evaluation of differential chemical effector responses across species and coupled with *in vivo* assays, the species-selective contributions of CAR in normal physiology and in disease processes such as hepatocarcinogenesis.

Key Words: **constitutive androstane receptor; liver; human; mouse; rat; dog.**

The constitutive androstane receptor (CAR; NR1I3) is a member of the nuclear hormone receptor superfamily and expressed primarily in the liver (Dekeyser and Omiecinski, 2010). Along with PXR (NR1I2), CAR functions as a xenosensor and transcriptional regulator of genes encoding all three phases of drug metabolism (Dekeyser and Omiecinski, 2010; Pascussi *et al*., 2008). A wide range of exogenous substances have been identified that activate these receptors, events that often result in altered pharmacokinetic profiles for many clinically important medications as well as in modified rates of either detoxication or bioactivation of environmental chemicals (Dekeyser and Omiecinski, 2010; Pascussi *et al*., 2008). In addition, both CAR and PXR have been established as key physiological regulators, affecting processes such as lipid homeostasis, glucose and energy metabolism, and bile acid elimination (Echchgadda *et al*., 2007; Gao and Xie, 2010; Maglich *et al*., 2004; Maglich *et al*., 2009). CAR is novel among the nuclear receptors in that it is constitutively active, in part due to its shortened activation function-2 (AF-2) helix and specific hydrogen bonding interactions that contribute to the docking of the AF2 helix in a position capable of interacting with nuclear coactivator proteins in the absence of ligand (Suino *et al*., 2004; Xu *et al*., 2004). In liver hepatocytes,CAR is typically tethered to a cytosolic complex that includes heat shock protein 90 and other chaperones. Chemical ligands as well as indirect non-ligand activators of CAR function to stimulate receptor dephosphorylation and release from the complex, resulting in subsequent nuclear translocation and receptor interaction with nuclear accessory proteins and gene targets (Mutoh *et al*., 2009). For example, the heterodimerization receptor, retinoid X receptor (RXR) α, is recruited to heterodimerize with CAR in the nucleus (Mutoh *et al*., 2009; Xu *et al*., 2004), and the resulting complex may bind to any of several DNA motifs (Frank *et al*., 2003). Direct repeat (DR)-4 and DR-3 motifs are specifically associated with the more proximal phenobarbital (PB)-responsive enhancer module (PBREM) and far upstream xenobiotic-responsive enhancer module (XREM), respectively, located in the regulatory region of genes such as CYP2B6 (Sueyoshi and Negishi, 2001; Wang *et al*., 2003).

Typically, nuclear receptors across vertebrate species exhibit high sequence conservation in their respective ligand-binding domains (LBDs) (Reschly and Krasowski, 2006). However,

CAR exhibits unusually low sequence conservation in these respects, even when comparing amino acid residues within the ligand-binding pocket (LBP) that are in direct contact with ligands (Reschly and Krasowski, 2006; Shan *et al*., 2004; Suino *et al*., 2004; Xu *et al*., 2004). These properties contribute toward species-specific ligand selectivity and gene targeting. For example, 6-(4-chlorophenyl)imidazo[2,1-*b*][1,3]thiazole-5-carbaldehyde *O*-(3,4-dichlorobenzyl)oxime (CITCO) is a selective ligand for human CAR, (Maglich *et al*., 2003), whereas 1,4-bis-[2-(3,5,-dichloropyridyloxy)] benzene (TCPOBOP) is selective for mouse CAR (Tzameli *et al*. (2000). On the other hand, androstanol (5α-androstan-3α-ol) is an inverse agonist for both human and mouse CAR(Forman *et al*., 1998). A recent study comparing mice that were humanized for CAR expression versus wild-type mice reported that overlapping but also distinct gene sets were transcriptionally activated in mouse liver by the respective species' CARs (Ross *et al*., 2010). These comparisons are especially relevant in view of the ability of PB, an indirect activator of both mouse and human CAR, to function as a promoter of hepatocarcinogenesis in mouse but not in humans (Holsapple *et al*., 2006; Ross *et al*., 2010).

Another confounder in the analysis of CAR function across species is the discovery of splice variation in human CAR. The CAR2 and CAR3 splice variants together appear to account for perhaps up to one third of the total CAR transcript pool present in human hepatocytes and are predicted to encode functional receptor proteins (Auerbach *et al*., 2003; Dekeyser *et al*., 2009). Further, both CAR2 and CAR3 have the significant property of encoding ligand-activated receptors that are not constitutively active, in contrast to the wild-type receptor, CAR1 (Auerbach *et al*., 2003; Dekeyser *et al*., 2009). Of these variants, whereas CAR2 demonstrates distinctive ligand activation profiles (Dekeyser *et al*., 2011), CAR3 appears to possess a ligand selectivity modeling that of wild-type receptor (Auerbach *et al*., 2005; Faucette *et al*., 2007).

In this study, we hypothesized that analogs of the naturally occurring human CAR3 receptor could be constructed across other mammalian species' forms of CAR that would similarly eliminate the constitutive activity of the wild-type CARs, yet preserve species-specific ligand-activated responses. Indeed, a battery of CAR3 variant receptors were successfully produced in mouse, rat, and dog and evaluated along with their wild-type and human receptor orthologs in mammalian cell-based assays. These analyses permitted identification and quantification of both agonist and inverse agonist responses that were uniquely reflective of species-selective profiles of CAR ligand interactions.

MATERIAL AND METHODS

Chemicals. Dimethyl sulfoxide (DMSO), clotrimazole (CLOT), artemisinin (ART), meclizine (MECL), itraconazole (ITRA), and 5α-androstan-3α-ol (ANDR) were obtained from Sigma (St Louis, MO). CITCO was purchased from BIOMOL Research Laboratories (Plymouth Meeting, PA). PB was obtained from the Division of Drug Services at the University of Washington Medical Center (Seattle, WA). TCPOBOP was obtained from the Environmental Chemistry Laboratory at the University of Washington (Seattle, WA). Etaconazole was obtained from Syngenta Ltd. (Bracknell, U.K.) and cervistatin was from Indigo Biosciences, State College PA). Primers for PCR and mutagenesis were purchased from Integrated DNA Technologies (Coralville, IA). COS-1 cells were purchased from ATCC (Manassas, VA).

Plasmids. The vectors pTracer CMV2-hCAR1, pcDNA 3.1-RXRá, and pGL3- basic/TK CYP2B6-dervied XREM/PBREM were described previously (Auerbach *et al*., 2007). pTracer CMV2-hCAR3 was also reported previously (Auerbach *et al*., 2005). Mouse, rat, and dog CAR3 mutant plasmids were constructed in our laboratory. Reference CAR for mouse and rat were amplified from existing plasmids and dog was amplified from RNA obtained from Zyagen Inc. (San Diego, CA). RNA was converted to complementary DNA (cDNA) using the Applied Biosystems High Capacity cDNA Reverse Transcription kit (Applied Biosystems, Foster City, CA) following the manufacturer's protocol. The mutant plasmids were constructed using either three-step PCR with Accusure taq polymerase (Bioline, Taunton, MA) or the QuikChange site-directed mutagenesis kit (Stratagene, La Jolla, CA) according to the manufacturer's protocol, then cloned into the pTracer CMV2 vector (Invitrogen, Carlsbad, CA) using EcoR1/EcoRV restriction sites. Primers are listed in Supplementary Table 1. The resulting plasmid constructs were verified by DNA sequencing. The sequences cloned into the respective expression vectors represented only the protein coding regions and were preceded by a Kozak sequence (Kozak, 1987). pRL-CMV, the expression plasmid encoding *Renilla* luciferase, was purchased from Promega (Madison, WI) and used in the Dual-Glo (Promega) assay system according to the manufacturer's protocol to normalize for transfection efficiencies in cultured cells. Prior to transfection, plasmids were prepared using the Qiagen Plasmid Plus Midi Kit (Qiagen, Valencia, CA).

Bioinformatics. Protein sequences were retrieved from the NCBI database. Amino acids 212–348 of the human CAR1 protein (NCBI RefSeq no. NP_005113.1) were used as the reference sequence and aligned using the blosum matrix of the ClustalW2 program. Genomic alignments used the University of California Santa Cruz (UCSC) genome browser (http://genome.ucsc.edu/) with the human *CAR* gene as the reference sequence. Comparative analysis of all the currently available vertebrate sequences for the CAR gene were performed to assess the CAR3 splice junction region existing at the 3′ end of intron 7, immediately upstream of the normal splice acceptor site at the beginning of exon 8.

Molecular modeling. The Phyre modeling program was used to generate a CAR3 LBD model. The structures of the LBPs of CAR1 and CAR2 were then characterized using the Pocket-Finder (http://bmbpcu36.leeds.ac.uk/pocket-finder/) (Laurie and Jackson, 2005). Models were visualized using the Deep View Swiss-PDB viewer v3.7 (http://ca.expasy.org/spdbv/) (Guex and Peitsch, 1997) for the predicted pockets, and the ICM MolSoft Browser v3.6.1 (http://www.molsoft.com/) was used to generate the CAR3 predicted structures and CAR1 structure.

Reporter assays. COS-1 cells (Simian virus-40–transformed green monkey kidney cells) were maintained in Dulbecco's modified Eagle's medium (DMEM) plus GlutaMAX-I with 10% fetal bovine serum (FBS), 10mM 4-(2-hydroxyethyl)-1-piperazineethanesulfonic acid (HEPES), 1mM sodium pyruvate, 1× non-essential amino acids, and 1% penicillin/streptomycin. All cell culture reagents were purchased from Invitrogen. For transfections, all media components remained the same except the FBS was replaced with 10% dextran/charcoal-treated FBS (HyClone, Logan, UT). The details of the luciferase reporter assays were described previously (Auerbach *et al*., 2005; Auerbach *et al*., 2007). Briefly, approximately 1 h prior to transfection, cells were trypsinized and plated onto 48-well plates (~50,000 cells per well). For determination of transcriptional activity of the hCAR constructs, cells were

transfected using Fugene 6 (Roche) according to the manufacturer's recommendations with a cotransfection plasmid mix consisting of 10 ng pRL-CMV (*Renilla* luciferase; Promega) for normalization, 25 ng pcDNA 3.1-RXRá, 100 ng of pGL3-basic/TK XREM/PBREM luciferase reporter plasmid, and 25 ng of either empty expression vector or the pTracer vectors containing the various CMV2-CAR expression constructs.

Each condition was performed in quadruplicate. All test chemicals were evaluated at 1, 10, and 30μM concentrations for each construct including the negative empty vector control. DMSO was used as a solvent control. A positive control assay with a model CAR activator for each construct was used at a single concentration. Luciferase assays were performed using the Dual-Glo Reporter Assay System (Promega) and a Veritas Microplate Luminometer (Turner Biosystems, Sunnyvale, CA). The Promega CellTiter-Glo Luminescent Cell Viability Assay was used to assess the toxicity potential of the itraconazole treatments over the extended dose range employed in these studies. At the highest dose employed, 30μM, cell viability was typically > 90%.

Statistical analyses. Firefly (*Photinus pyralis*) luminescence data values were recorded for each replicate and normalized luciferase activities were then calculated by dividing the raw luciferase values by the *Renilla* luciferase signals in order to correct for any differences in transfection efficiency among the COS-1 cell assay wells. Data are expressed as means ± SD ($n = 4$). Quantitative data were examined by one-way ANOVA followed by Dunnett's *post hoc* test to compare all groups with the DMSO control. Significance was declared if $p < 0.01$. All statistical analyses were performed using GraphPad Prism v5.03 for Windows (GraphPad Software, San Diego, CA).

Human hepatocytes. Enriched primary human hepatocyte cultures plated on collagen were obtained through the Liver Tissue Procurement and Distribution System, University of Pittsburgh, funded by National Institutes of Health (NIH) Contract # N01-DK-7-0004/HHSN267200700004C. Cells were placed in fresh William's E media containing: 1% penicillin-streptomycin, 1% HEPES, 20μM glutamine, 25nM dexamethasone, 10nM insulin, 1% linoleic acid/bovine serum albumin, 5ng/ml selenious acid, and 5μg/ml transferrin, as described previously (Sidhu *et al*., 2004). The cells were harvested in TRIzol (Invitrogen) 24 h after treatment, and RNA was isolated following the manufacturer's protocol. After 48 h, the treated hepatocytes were harvested in NP-40 lysis buffer (20mM Tris, pH 7.5; 100mM NaCl; and 0.5% NP-40) followed by sonication to permit isolation of total cellular protein fractions.

Quantitative real-time PCR. cDNA was prepared from 2 μg of total hepatocyte RNA using the High Capacity cDNA Reverse Transcription Kit (Applied Biosystems) following the manufacturer's protocol and diluted to a final concentration of 20 ng/μl. Reaction components were prepared for duplicate 25 μl reactions in 96-well plates: 2× PerfeCTa SYBR Green SuperMix, UNG, ROX (Quanta Biosciences, Gaithersburg, MD), 25 μl; 5μM forward and reverse primers (Supplementary Table 2), 1.0 μl each; cDNA, 5 μl; and RNase-free water, 18.0 μl. Samples were mixed and then split into individual wells. Using the Applied Biosystems 7300 Real-Time PCR System, plate documents were configured with the appropriate assay and sample information. Thermocycling conditions were as follows: UNG activation, 5 min at 45°C, hold 3 min at 95°C, and for each of 40 cycles, 15 s at 95°C and 1 min at 60°C. A dissociation stage was added to determine specificity of the primers (15 s at 95°C, 30 s at 60°C, and 15 s at 95°C). Sequence Detection System software (ABI) was used to collect and organize the fluorescence data for analysis. Instrumentation data were collected at the same cycle threshold (C_t) level for each sample within the logarithmic phase of the amplification reaction and analyzed using the $\Delta\Delta C_T$ method (Livak and Schmittgen, 2001; Page *et al*., 2007). Results were expressed as fold change over control samples.

Western blot. Ten micrograms of total protein were heated at 95°C prior to loading onto a precast 10% Tris-HCl sodium dodecyl sulfate-polyacrylamide electrophoresis (SDS-PAGE) gel (Bio-Rad). As previously described (Page *et al*., 2007), proteins were separated by denaturing SDS-PAGE (100 V for 1.5 h in 0.03M Tris, 0.2M glycine, and 0.025% SDS) and electrophoretically transferred to polyvinylidene fluoride membranes (120 V for 1 h in 0.03M Tris, 0.2M glycine, and 20% methanol). Membranes were blocked in 5% nonfat dry milk and Tris buffer saline (TBS)-T (0.1% Tween) for 1 h prior to the addition of primary antibody diluted in blocking buffer. Mouse monoclonal antibodies directed against human CYP2B6 and CYP3A4 were obtained from the Laboratory of Metabolism, National Cancer Institute/NIH and were diluted 1:1000 prior to use. Membranes were incubated with primary antibody overnight at 4°C with rocking and then washed three times for 5 min each in TBS-T. Membranes were then incubated with the appropriate secondary horseradish peroxidase–conjugated antibody diluted 1:5000 in blocking buffer for 1 h at 25°C with rocking. After three 5-min washes in TBS-T, protein-antibody complexes were visualized by chemiluminescence (Pierce Supersignal West Pico Chemiluminescent Substrate; Thermo Scientific, Rockford, IL) and exposure to x-ray film.

RESULTS

Comparative Genomic Analysis of the CAR3 Splice Junction

As the CAR3 splice variant was initially identified in human messenger RNA (mRNA) samples, using the UCSC genome browser we performed a comparative analysis of all the vertebrate genomic sequences currently available for the *CAR* gene, with specific focus on the CAR3 splice junction region existing at the 3′ end of intron 7, immediately upstream of the normal splice acceptor site at the beginning of exon 8. The data are presented in Figure 1. The boxed area in the figure indicates the respective comparative genomic sequences. In this context, an alternative "AG" splice acceptor site is apparent in 9 of the 19 genomic sequences available in the database; however, one of these, the mouse, is missing two nucleotides at the 3′ end of the alternative junction region and thereby use of this alternative splice acceptor would be predicted to produce an out-of-frame and nonfunctional mouse CAR protein. Rat and dog are included in a list of species not possessing the alternative AG CAR3 splice acceptor site. It is noteworthy that all primate species do possess the alternative site as does guinea pig. Of the eight species with the AG site, five are predicted capable of producing a CAR3 protein with the exact "APYLT" amino acid insertion as human, whereas the rabbit, marmoset, and bush baby are predicted to produce an altered 5-amino acid (aa) insertion. Independent analysis of the African Green Monkey genomic sequence also revealed the presence of the exact same structure as human within this region, thereby predicting the latter species is also capable of producing the CAR3 variant (data not shown). Additional studies were conducted to assess CAR transcripts in both rabbit and guinea pig liver; however, the CAR3-like transcript was not detectable in either of these latter two species (data not shown).

Ligand-Binding Domain

The predicted CAR3 model is shown superimposed on the CAR1 structure in Figures 2A and 2B. The main chain coordinates of the CAR structures are very similar, with the exception of the amino acids flanking the APYLT CAR3 insertion (indicated in yellow in panels A and B). Ramachandran analysis showed that 86.3% of the residues were in favored regions, 11.2% were in allowed regions and 2% were in outlier regions. One outlier was an arginine (R277) that was

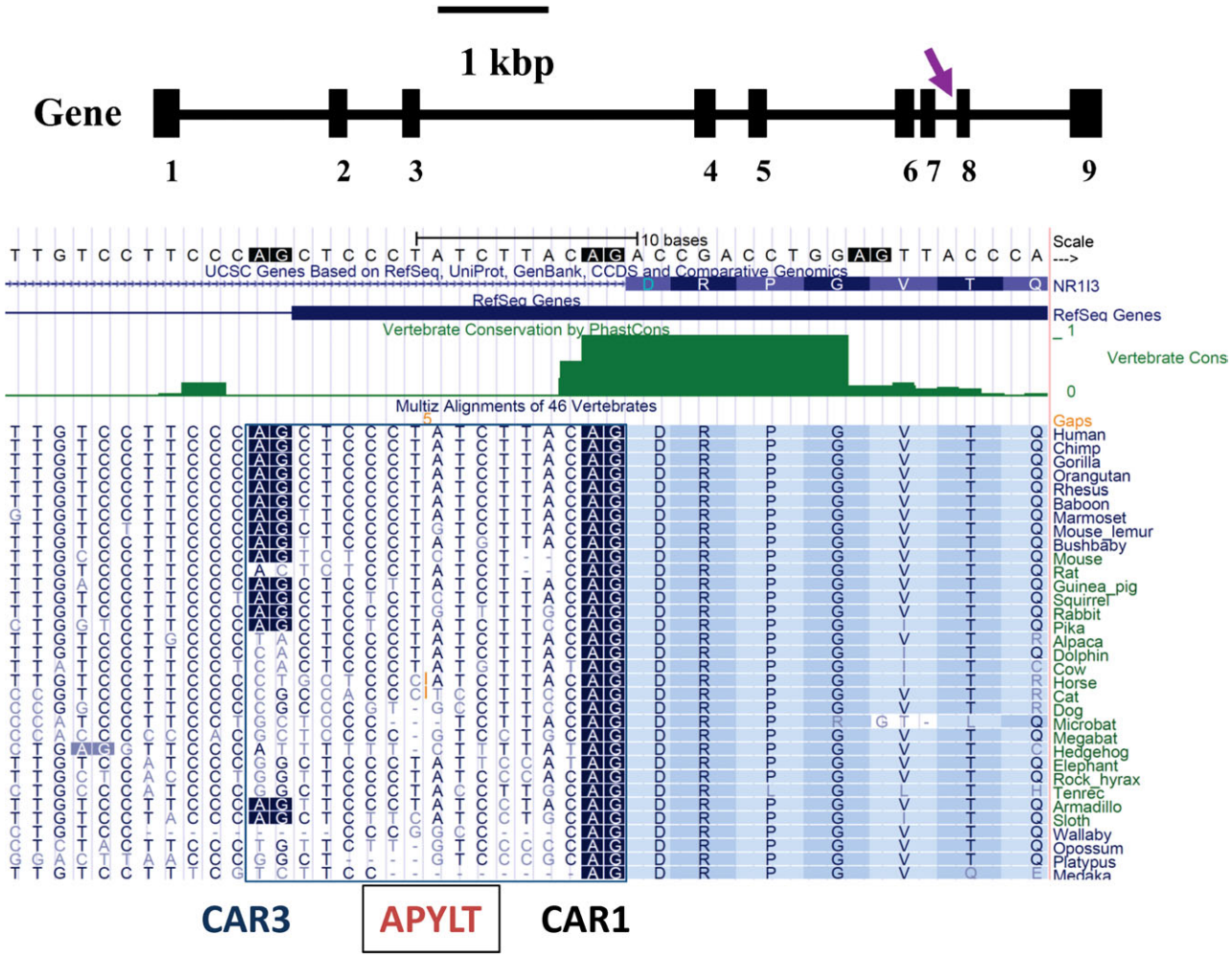

FIG. 1. Genomic sequence comparisons of CAR3 (Nr1I3) alternative exon usage in 33 vertebrate species. The UCSC genome browser was used to identify sequence conservation features among the CAR3 splice junction site within the region immediately 5′ of exon 8. The upper portion of the figure depicts the overall *CAR* gene structure, with exons indicated by black boxes. The region of detailed analysis is shown via the purple arrow. The alignments are referenced to the human *CAR* gene. The sequence conservation among the comparative vertebrate species is indicated by green tracing labeled ''Vertebrate Cons'' in the upper portion of the figure. ''Gaps,'' indicated in orange, refers to the number of nucleotide bases that the browser needed to insert to obtain best sequence alignment among the species. The dark blue box brackets the region containing potential alternative ''AG'' splice acceptor sites (highlighted in blue), giving rise to either the reference protein, CAR1, or to the CAR3 protein that in human possesses the additional 5-aa motif, ''APYLT.'' The reader is referred to the ''Results'' section of the manuscript for additional description of the figure.

a pre-proline residue, two residues away from the carboxy-end of the APYLT insertion. Space filling models of the predicted CAR1 and CAR3 LBPs are shown in Figures 2C and 2D. The calculated pocket volume (701 $Å^3$) of CAR3 was virtually identical to the pocket volume predicted for CAR1, an anticipated result because the APLYT insertion lies between helices 8 and 9, and therefore is not expected to affect the LBP.

CAR3 Variants/Mutants Exhibit Negligible Constitutive Activity Allowing for More Sensitive and Differential Screening

In this study, we humanized the mouse, rat, and dog CAR1 receptors to their corresponding CAR3 variant forms by inserting the respective 15 bp/5-aa of the human CAR3 sequence in the same exon 7/8 junctions of these species' receptors (see Fig. 1 for reference). Each species' CAR1 and CAR3 variant receptors were evaluated in mammalian cell, COS-1-based transfection assays using a luciferase reporter driven by a PBREM/XREM response element derived from the endogenous human CYP2B6 gene (Auerbach *et al.*, 2005; Wang *et al.*, 2003). Similar results to those reported here for the CAR1 assays were also obtained in separately conducted reporter assays using these agents in human hepatoma-derived HepG2 as well as Huh7 cell cultures (data not shown). As can be seen by comparing all the left side panels of Figure 3 (A,C,E, and G) with those of the right side panels (B,D,F, and H), the reference form of CAR (CAR1) from human, mouse, rat, and dog exhibits

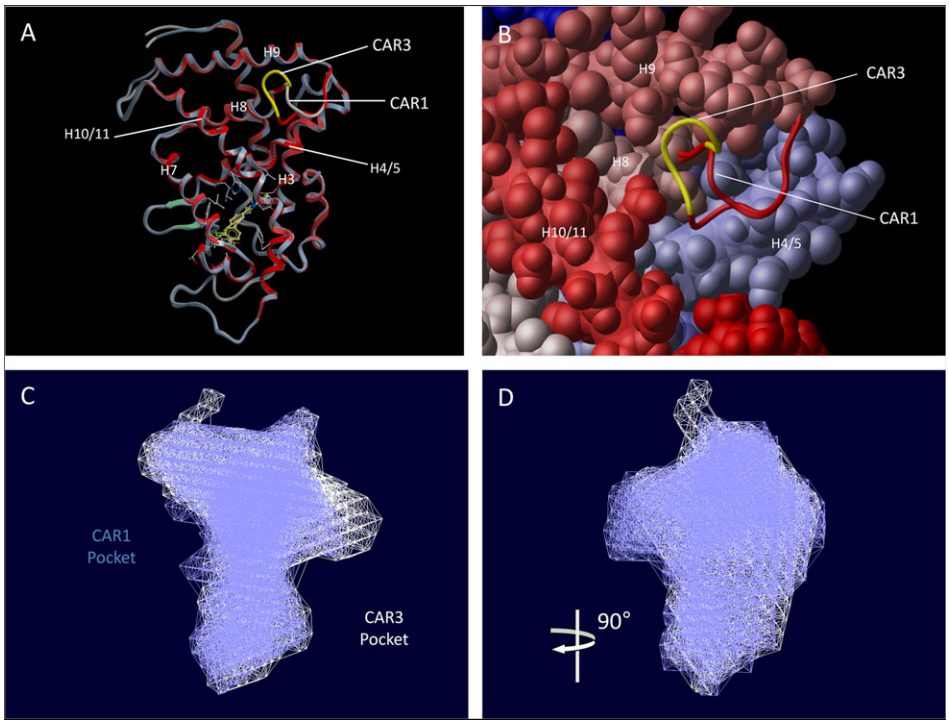

FIG. 2. Comparative molecular modeling predictions of CAR1 and CAR3 structures. The ICM Molsoft Browser v.3.6.1 was used to view the respective structures presented in panels A and B. Panel A shows a ribbon structure superimposition of the predicted CAR1 and CAR3 ribbon structures, based on the crystal structure coordinates published for human CAR1 (1XVP.pdb) and the structural model predictions for CAR3 obtained from the Phyre algorithm (Protein Homology/Analogy Recognition Engine; http://www.sbg.bio.ic.ac.uk/phyre/). The RXR dimer interface view is being visualized. The ligand CITCO (yellow) is shown within the ligand binding pocket of the CAR1 crystal structure. Panel B illustrates a zoomed space-filling model, obtained identically as described for Panel A. In panels C and D, space filling models of the respective CAR1/CAR3 ligand binding pockets are presented, superimposed but viewed from different 90 degree perspectives in the respective panels. The Pocketfinder algorithm (http://bmbpcu36.leeds.ac.uk/pocketfinder/) was used to develop the modeling predictions. The Swiss-PDB viewer v.3.7 was used to generate the images in panels C and D.

high constitutive activity across each species. While the graphs in Figure 3 show the fold-change relative to control (set to 1.0), the actual normalized luciferase activities were much lower in the CAR3 variant receptor (e.g., 0.01 in mCAR3) compared with the background constitutive activity in CAR1 (e.g., 1.64 in mCAR1), as seen in Supplementary Table 3. This high level of constitutive activity in cell-based assays obscures the detection of ligand activators as shown in the left side panels of Figure 3. In contrast, the natural human CAR3 splice variant has been characterized as possessing negligible constitutive activity but is responsive to direct CAR ligand activators (Auerbach *et al.*, 2005; Faucette *et al.*, 2007), although not indirect activators such as PB within *in vitro* assay systems. The respective species responses for the CAR1- and CAR3-derived receptors were evaluated following exposures to nine different chemical agents, a battery that included the previously reported CAR ligand activators, CITCO and TCPOBOP, for human and mouse CAR, respectively (Maglich *et al.*, 2003; Tzameli *et al.*, 2000) and an indirect activator, PB, of human, mouse, and rat CAR (Lamba *et al.*, 2005). Additional compounds tested among the nine agents have been less consistently documented in terms of species-specific CAR activation and included the reported human CAR inverse activators, CLOT and meclizine (Huang *et al.*, 2004b; Moore *et al.*, 2000); an HMG-CoA reductase inhibitor, cervastatin, reported as an activator of human, mouse and rat CAR (Kobayashi *et al.*, 2005); the antimalarial drug, artemisinin, reported as an activator of both human and mouse CAR (Burk *et al.*, 2005; Faucette *et al.*, 2007); and two antifungal conazole derivates, etaconazole (a triazole) and itraconazole (ITRA; an imidazole) that have not been evaluated previously as CAR activators.

As indicated, in particular from viewing the right side panels of Figure 3, the respective CAR3 mutants exhibited anticipated species-specific responses to the battery of test chemicals. For example, CITCO exerted marked activation with human CAR3 but only minimal effects with mouse CAR3 (Figs. 3B and 3D), whereas TCPOBOP markedly activated mouse CAR3 while only exhibiting minimal effects on human CAR3 (Figs. 3B and 3D). PB showed no activation in human, mouse or rat CAR3, as expected for an indirect activator.

Although the prototypical CAR effectors, PB, CITCO, and TCPOBOP, were evaluated at a single dose, dose-response relationships were determined for five of the test chemicals, assayed at 1, 10, and 30μM. As previously reported and therefore anticipated, meclizine exhibited strong activation of mouse CAR but not human CAR. Meclizine did not activate human CAR1,

dog CAR1, or dog CAR3; however, it activated human CAR3 activity approximately twofold to fourfold, and mouse CAR1 and CAR3 activity were significantly induced at all doses, with mouse CAR3 dose dependently activated from 5- to 37.4-fold (Fig. 3D). In some contrast, rat CAR1 was activated by this agent only slightly at 10 and 30μM, while rat CAR3 demonstrated approximately fivefold activation at 30μM meclizine.

A number of other relevant species-selective results were evident from these studies. For example, of the agents tested, CLOT was the most potent activator of rat CAR3 (Fig. 3F), whereas artemisinin was the most notable activator of dog CAR3 (Fig. 3H)—a result also apparent in the parallel dog CAR1 assays (Fig. 3G).

Etaconazole activated rat CAR3 by 12- to 23-fold and had only a slightly lower activity in activation of mouse CAR3 (9- to 16-fold) at 10 and 30μM, but there was no activation of dog CAR3. The response with human CAR3 was only statistically significant at 30μM and represented a modest 2.6-fold increase.

Cervistatin did not produce activation of CAR3 complexes in any of the four species at concentrations up to 30μM. This lack of responsiveness is in contrast to a reported increase suggested in reporter assays utilizing the native forms of human, rat, and mouse CAR with cervistatin and several other HMGCoA-reductase inhibitors (Kobayashi *et al*., 2005). A much larger fold-activation was observed by Kobayashi *et al*. in a human PXR transactivation assay in comparison to the small increases in their CAR transactivation assays, and therefore, the results with the more sensitive CAR3 assays shown here support the concept that the statins may operate more exclusively as PXR activators.

Of particular interest, ITRA, an agent not previously assessed for CAR response, exhibited marked inverse agonism activity relative to the DMSO vehicle control in each species examined. These responses were most evident when viewing the results of the respective CAR1 assays, as in the CAR3 multispecies assessments the larger fold-change of other activators caused the right-side panels in Figure 3 to be displayed on a much larger y-axis scale. However, examination of actual fold-change values (Supplementary Table 3) shows that a concentration-responsive decrease in fold-change occurred with mCAR3 and rCAR3 that was only slightly lesser in magnitude than the effect of inverse agonism seen with ITRA in mCAR1 and rCAR1. With dCAR3 and hCAR3, the decreases in fold-change values for ITRA that had been seen in the corresponding CAR1 assays were not apparent. These results as well as the clinical toxicity reported for ITRA (Song and Deresinski, 2005), prompted us to further evaluate the nature and effects of ITRA in various experimental models.

Competition Assays Using the CAR1 and CAR3 Variant/Mutant Can Be Used to Assess Inverse Agonists

The studies conducted in Figure 3 identified ITRA as a potential inverse agonist of the reference form of CAR in each species assayed. To better characterize this potential activity, we used a series of competition assays conducted in the same transfection/reporter assay system as conducted for the results presented in Figure 3. Androstanol is a known potent inverse agonist of CAR and is used commonly in competition assays to assess potential ligands of CAR1 (Forman *et al*., 1998). In this study, we used androstanol as a control to study potential inverse agonist ability of ITRA. In the panels on the left side of Figure 4, we assessed the abilities of dose-dependent titration of the most effective chemical activators identified for each species CAR3s, namely, CITCO (human), TCPOBOP (mouse), CLOT (rat), and artemisinin (dog), to compete with the inverse agonists, ITRA or androstanol, when the latter were present at a fixed concentration in the cell cultures. To enable functional visualization of the inverse agonism responses, all the studies shown were conducted with the respective CAR1 forms of each species' receptor.

Initially apparent from the data, single additions of either ITRA or androstanol produced marked inhibition (inverse agonism) of the constitutive activities otherwise associated with each species' CAR1s (Fig. 4, left-side panels). In the fixed presence of either inhibitor, the titration of CAR1 agonists resulted in largely dose-dependent restoration of the respective CAR1s' constitutive activity (Figs. 4A, 4C, 4E and 4G). ITRA's receptor antagonism was completely reversed in the mouse by TCPOBOP at 0.5μM, and it was largely reversed in the other species CAR1 responses as well, using the respective activators for each of those species. The inhibition by androstanol of CAR1 activity was comparatively more difficult to reverse with agonist additions, especially in mouse and dog (Figs. 4C and 4G), but readily reversible in human and rat (Figs. 4A and 4E), indicating species differences in the affinity of androstanol interactions across their respective CARs.

The converse experiments were conducted in the assays whose results are presented on the right side of Figure 4. These studies were performed with the CAR3 constructs to allow visualization of agonist inhibition. Either ITRA or androstanol were titrated into the reporter assays, with the levels of chemical activator remaining fixed. In each species, a dose-dependent inhibition of the agonist activities was evident when adding either ITRA or androstanol, with one exception in which concentrations of up to 10μM androstanol did not clearly produce an inhibitory effect in human CAR3. Together, the data from the ITRA results depicted in Figures 3 and 4 support the contention that this agent is a potent inverse agonist of the CAR receptors of at least four species of vertebrates.

Effects of Itraconazole in Primary Human Hepatocytes

Human hepatocytes were cultured as described in "Materials and Methods" and treated with selected CAR activators and with differing doses of ITRA either alone or in combination with 1μM CITCO. Resulting protein levels for CYP2B6 and CYP3A4 (Fig. 5, panel A) and quantitative real-time PCR

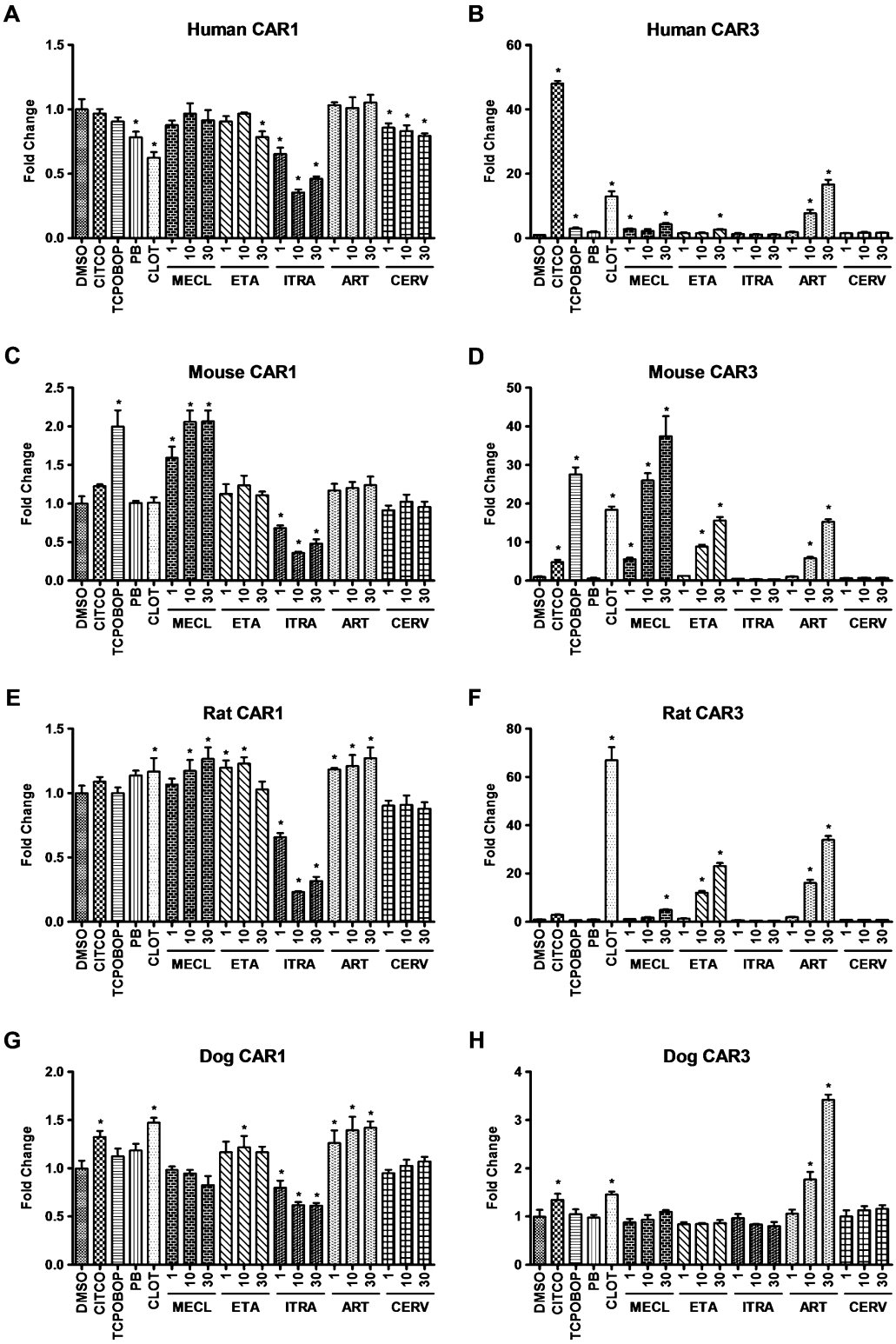

FIG. 3. Comparative multispecies CAR1 and CAR3 reporter assays conducted with prototypical and experimental ligands. The CAR3 variants created in each of the respective species exhibit negligible constitutive activity allowing for detection of chemical dose-response relationships that are not apparent in the CAR1 assays. Species selective CAR ligands were used as controls (human, 5μM 6-(4-chlorophenyl)imidazo[2,1-b][1,3]thiazole-5-carbaldehyde O-(3,4-dichlorobenzyl)oxime (CITCO); mouse, 0.5μM 1,4-bis-[2-(3,5,-dichloropyridyloxy)] benzene (TCPOBOP); rat, 10μM clotrimazole (CLOT); and dog, 10μM CLOT). The indirect CAR activator phenobarbital (PB) was tested at a single concentration (500μM) and was predicted not to be functional in this direct CAR activation assay. The remaining test chemicals, meclizine (MECL), etaconazole (ETA), itraconazole (ITRA), artemisinin (ART) and cervistatin (CERV), were each

assays measuring transcript levels (Panels B and C) were assessed. The data obtained from the immunoblot experiment demonstrate the induction of both CYP2B6 and CYP3A4 protein following exposures to CITCO or PB (Panel A). Increasing concentrations of ITRA were ineffective at inducing the respective proteins. Additions of increasing concentrations of ITRA along with 1μM CITCO resulted in a markedly diminished level of detection of both the CYP proteins. Similar results were obtained in experiments conducted with hepatocyte preparations derived from three separate donors (data not shown). These results are largely consistent with the dramatic downregulation of ITRA treatments on the respective mRNA transcript levels for the respective CYPs after 24 h of incubation (Fig. 5, Panels B and C) and further support the identification of CAR as a selective and potent target for ITRA. It is noteworthy that ITRA not only inhibited induced activities of CAR but also repressed basal levels of CAR target gene expression. These results suggest that CAR in human hepatocytes may play a role in basal regulation of CAR target genes, although potential effects of ITRA on other pathways in these respects cannot be excluded.

DISCUSSION

A large number of pharmaceutical compounds, natural product constituents, and other xenobiotic chemicals have been identified as CAR activators (Chang and Waxman, 2006), establishing the importance of this receptor pathway as a key modulator of xenobiotic-induced toxicity and as an important mediator of physiological processes including lipid homeostasis and bile acid elimination (Dekeyser and Omiecinski, 2010). CAR is unusual among nuclear receptors in that it possesses high constitutive activity in the absence of ligand. Another unusual feature is that the receptor exhibits high sequence divergence among vertebrates in its LBD (Reschly and Krasowski, 2006) contributing to species-selective ligand binding profiles (Moore *et al*., 2003). In the liver or in primary hepatocytes, a number of direct acting ligands for CAR function as agonists, stimulating its nuclear translocation and subsequent interaction of the CAR-RXR-DNA complex with nuclear coactivator proteins. Conversely, other CAR ligands function as ''inverse agonists,'' a term reflecting the ability of ligands to downregulate the high level of receptor constitutive activity, presumably through disruption of coactivator interactions and recruitment of nuclear corepressors (Dussault *et al*., 2002). Due to its high levels of constitutive activity, examining potential CAR-ligand interactions in cell-based assays is compromised by issues that include high background and resulting low signal to noise ratios.

A further class of CAR chemical activators functions indirectly. PB is a hallmark example of an indirect activator that signals selectively through the CAR pathway (Moore *et al*., 2000; Scheer *et al*., 2008). Certain organochlorine insecticides such as chlordane as well as natural product extracts such as 6,7-dimethylesculetin appear to interact similarly as indirect CAR activators (Huang *et al*., 2004a; Ross *et al*., 2010). These nonligand CAR activators trigger nuclear translocation through pathways that appear to modulate the receptor's phosphorylation status, thereby disrupting its cytosolic tethering complex (Mutoh *et al*., 2009). Prolonged exposure at high dose levels to the indirect activator, PB, as well as the direct-acting mouse CAR activator, TCPOBOP, produce an increased incidence of hepatocellular adenomas and/or carcinomas in rodent livers *via* a non-genotoxic mode of action, a process that appears inextricably linked to CAR activation (Huang *et al*., 2005; Yamamoto *et al*., 2004). It is noteworthy that despite the presence of CAR in human liver and its marked activation by PB, results of several large epidemiological studies have demonstrated convincingly that PB does not elevate risks of hepatocellular tumors in humans, even in individuals maintained on PB for many years in the course of antiseizure therapy (Holsapple *et al*., 2006; Lamminpaa *et al*., 2002; Whysner *et al*., 1996). The high level of CAR sequence divergence among species likely accounts for both the different ligand specificities and gene activation effects associated with various species' CARs, and consequently, PB's differing tumor promoting potential in rodents versus man. For example, a recent report evaluated gene expression profiles between wild-type mice and transgenic mice that were humanized for both CAR and PXR. Upon activation with either PB or chlordane, wild-type mice exhibited upregulation of hepatic genes associated with both hypertrophic and hyperplastic responses, whereas humanized CAR/PXR mice exhibited only enhanced hypertrophic signatures, results consistent with the respective liver histopathologies produced (Ross *et al*., 2010).

CAR's biology in humans is further underscored with the identification of naturally occurring splice variants. Although perhaps 29 different variant RNA transcripts have been documented for human CAR (Arnold *et al*., 2004; Auerbach *et al*., 2003; Jinno *et al*., 2004; Lamda *et al*., 2005), many of these variants can likely be discounted as having low biological relevance due to either extremely low expression level and/or predicted production of aberrant and nonfunctional protein

←
evaluated at three doses: 1, 10, and 30μM. Transactivation assays were performed in COS-1 cells using CAR expression plasmids and a CYP2B6-derived PBREM/XREM luciferase reporter as indicated in the figure and as described under ''Materials and Methods''. Data are presented as fold change, setting the DMSO vehicle response as equal to 1. Each data point represents the mean ± SD of four separate transfections. Panels A, C, E, and G: transactivation of the reference form of CAR for each species. Panels B, D, F, and H: transactivation of the CAR3 variant form for each species. *Denotes data points that were significantly different from their respective DMSO control as determined by ANOVA in combination with a Dunnett's multiple comparison posttest ($p < 0.01$).

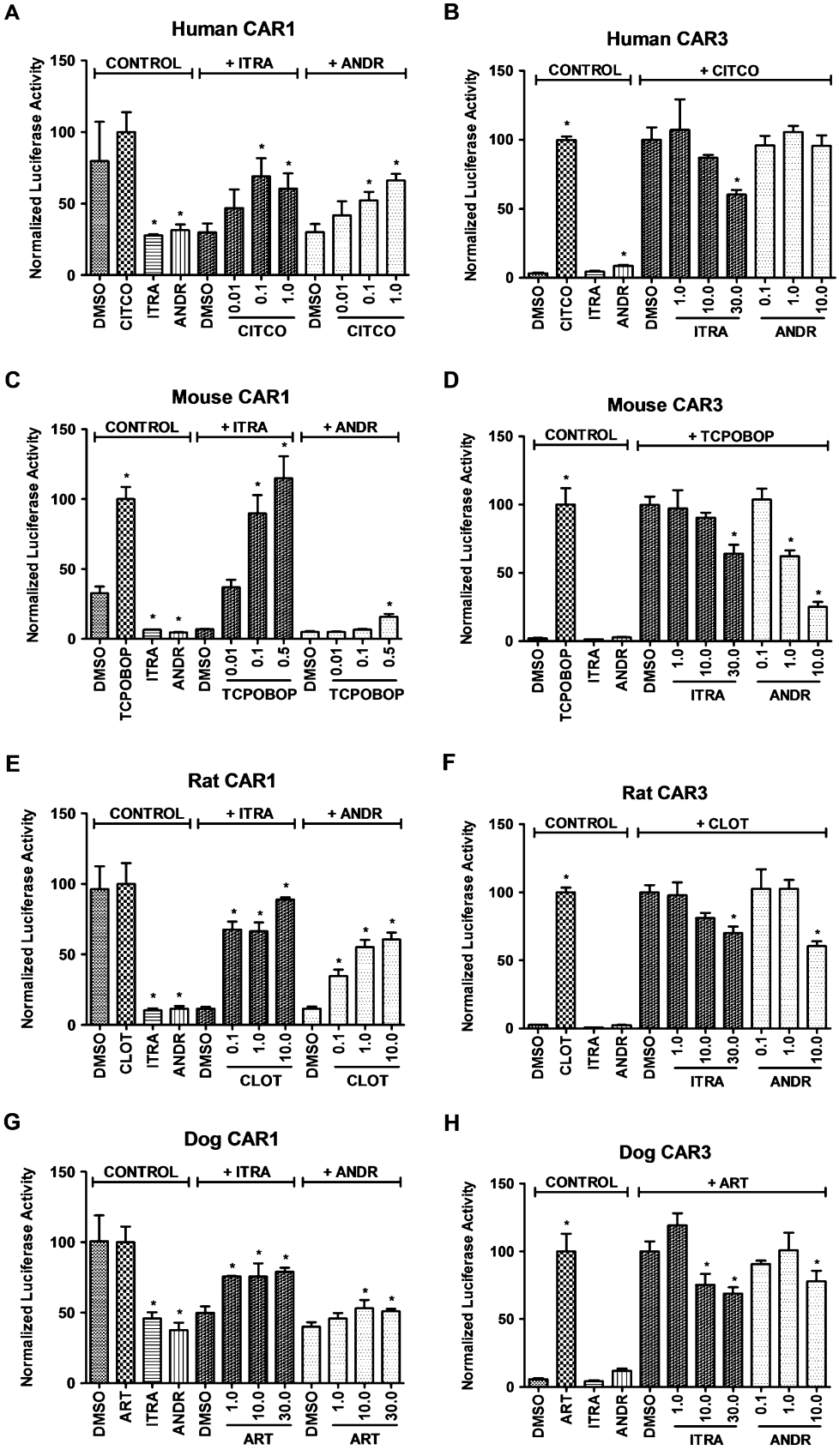

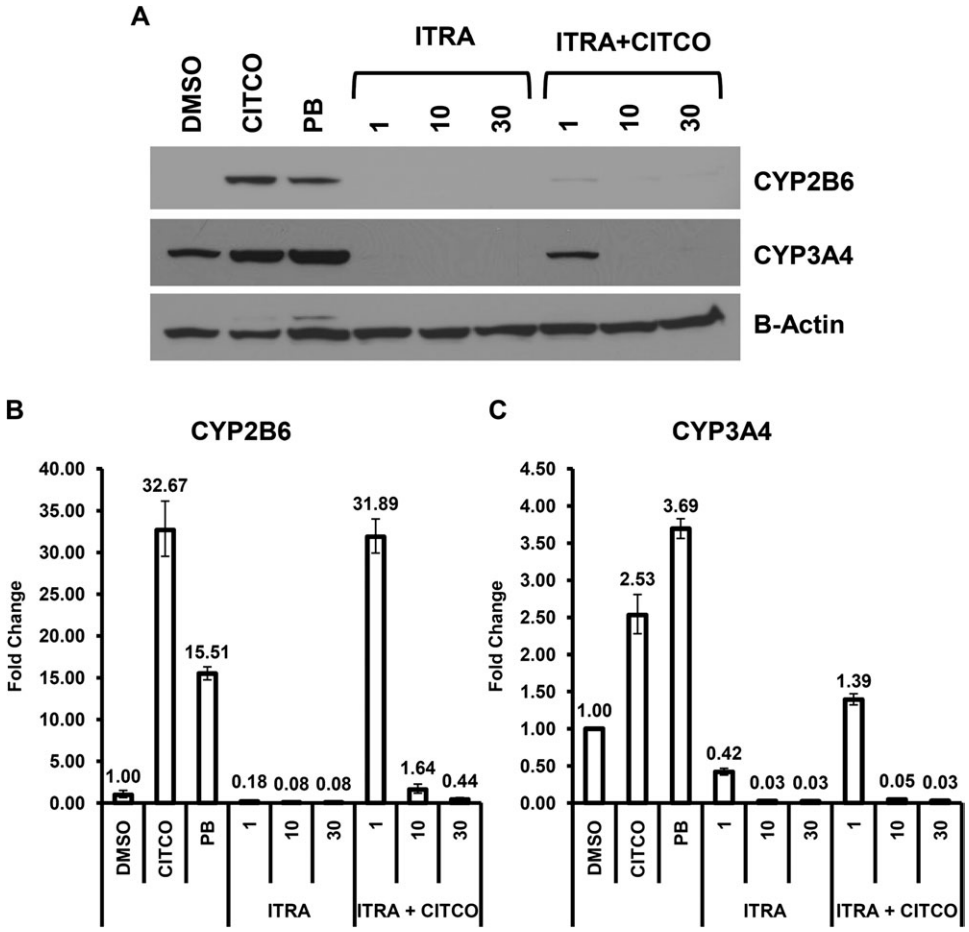

FIG. 5. Immunoblot and RT-PCR analyses of the effects of Itraconazole on CYP2B6 and CYP3A4 expression in primary human hepatocyte cultures. Primary human hepatocyte cultures were maintained and treated with chemicals as indicated in the ''Materials and Methods.'' Chemical treatments were as follows: DMSO; 1μM CITCO; 500μM PB; 1, 10, and 30μM itraconazole; and 1, 10, and 30μM itraconazole cotreated with 1μM CITCO. TRIzol fractions were collected after 24 h for mRNA analysis. Protein samples were collected after 48 h of treatment. Panel A shows the results of western blot analysis for both CYP2B6 and CYP3A4 using β-actin as a loading control. Panels B and C show the results of quantitative RT-PCR analyses assessing the corresponding mRNA levels for CYP2B6 and CYP3A4. The y-axis represents fold-change compared with the DMSO control for both CYP2B6 and CYP3A4, normalized to β-actin.

products. However, two CAR variants, termed CAR2 and CAR3, contain short 4- and 5-aa insertions, respectively, within their LBD/heterodimerization domain, and may represent up to a third of the total CAR pool in human liver (Auerbach *et al*., 2003; Dekeyser *et al*., 2009; Jinno *et al*., 2004; Ross *et al*., 2010). Unlike the constitutively active wild-type receptor, neither CAR2 or CAR3 are constitutively active, rather they are ligand-activated receptors.

Using the UCSC genome browser, we identified potential splice acceptor sites that might function to generate analogous CAR3 variant receptors in several other species, predominantly in primate species but also in guinea pig and rabbit (Fig. 1).

←

FIG. 4. Competition assays for potential inverse agonist using both CAR1 and CAR3 variants for each species. For CAR1, both itraconazole (ITRA) and androstanol (ANDR) were kept constant at 10μM; each species selective CAR ligand was then titrated using three doses, with DMSO serving as the control. For CAR3, the species-selective ligand concentration was kept constant (human, 1μM CITCO; mouse, 0.5μM TCPOBOP; rat, 10μM CLOT; and dog, 30μM ART), with additions of itraconazole and androstanol then titrated at three doses, with DMSO serving as control. Transactivation assays were performed in COS-1 cells using CAR expression plasmids and a CYP2B6-derived PBREM/XREM luciferase reporter as indicated in the figure and as described under ''Materials and Methods.'' Data are presented as normalized luciferase values within each separate treatment group, normalized to 100% responses obtained within that group by the most potent ligand activator identified for each species. Each data point represents the mean (± SD) of four separate transfections. Cell viability assays conducted with itraconazole indicated minimal toxicity of the agent even at the highest dose used (30μM) in these studies (data not shown). Panels A, C, E, and G: transactivation of the reference form of CAR for each species. Panels B, D, F and H: transactivation of the CAR3 variant/mutant for each species. * Denotes data points that were significantly different from their respective DMSO control as determined by ANOVA in combination with a Dunnett's multiple comparison posttest ($p < 0.01$).

However, in separate investigations (Coslo and Omiecinski, unpublished data), we were not able to detect orthologous CAR3-like (or CAR2-like) transcripts in liver tissues derived from either guinea pig or rabbit. These results point to differences that likely exist among splice site recognition and/or splicing machinery among species. Mouse, rat, and dog are considered incapable of generating CAR3-like isoforms, as the CAR locus in those species either do not contain the canonical AG splice acceptor motif in their respective genomic sequence contexts or they possess nucleotide deletions within the CAR3 insertion sequence that would result in the generation of out of frame and nonfunctional receptor proteins (Fig. 1). As presented in Figure 2, results of molecular modeling studies predict that the 5-aa insertion in CAR3 results in a receptor with virtually an identical LBP to that of wild-type CAR, suggesting that CAR3 may serve as unique surrogate for wild-type CAR in studies of ligand-specificity analyses. These modeling predictions for human CAR3 have been examined in functional assays reported previously (Auerbach *et al*., 2005; Faucette *et al*., 2007) and are further supported by the results presented in the current investigation. Interestingly, another recent report examined the functional activity of a CAR3-like receptor that possessed only the "A" residue of the naturally occurring CAR3 APYLT motif (Chen *et al*., 2010). These investigators demonstrated that the single A residue was sufficient to eliminate CAR constitutive activity and similarly conferred ligand activation functionality to the resulting receptor variant. That these seemingly subtle alterations in CAR structure lead to loss of the receptor's constitutive activity are likely due to the extension imposed by these residues in a loop region between helix 8 and helix 9 of the receptor (Fig. 2A and 2B), resulting in disruption of the receptor's normal AF2 domain positioning. Other single amino acid mutations in either mouse or human CAR result in similar disruption of AF2 domain positioning and loss of constitutive activity (Dussault *et al*., 2002; Suino *et al*., 2004; Xu *et al*., 2004).

In the studies presented here, we were successful in duplicating the naturally occurring human CAR3 variant within multiple mammalian species of CAR. These resulting CAR3 variants were deployed in expression studies to examine the context of chemical activation and inhibition responses with nine different agents representing both prototypical CAR effectors as well as other compounds whose activities as CAR modulators are less defined. We demonstrate that the derived CAR3 receptors retained species-selective response to select ligands (Fig. 3). Further, the CAR3 modified receptors enabled a much more sensitive and expanded view of the respective species-specific chemical interaction profiles.

Of note, we identified that the human imidazole antifungal agent, ITRA, as a potent inverse agonist of CAR in each species assayed, i.e., human, mouse, rat, and dog (Figs. 3 and 4). ITRA is a clinically employed antifungal agent, and its use has been associated with cholestatic liver injuries in patients as well as a number of patient deaths (Song and Deresinski, 2005). A recent report indicated that ITRA might inhibit the bile canalicular phospholipid transporter, MDR3/ABCB4 (Yoshikado *et al*., 2011). As bile transport is an important route of detoxication for cholesterol metabolites and certain bile acid transporters are targets of CAR-mediated induction, the results presented here might have clinical relevance as ITRA inhibition of CAR, coupled with compromised bile acid transport function might be a precipitating factor in ITRA toxicity. Another imidazole, CLOT, has previously been characterized as a human CAR inverse agonist (Moore *et al*., 2000), a result observed in the present study as well (Fig. 3A). However, it is interesting that CLOT also exhibited activation activity on human CAR3 (Fig. 3B), a result also observed previously in our CAR3 studies (Auerbach *et al*., 2005). Given that even CITCO may adopt differing conformations within the human CAR LBP (Xu *et al*., 2004) and that it is becoming increasingly recognized that ligand orientation may influence receptor conformation (Bruning *et al*., 2010), we suggest that the conformational interactions of CLOT within the various CAR LBPs under analysis in this study may impart allosteric change in the receptors' conformation, thus modulating the relative interactions with nuclear coactivators and/or corepressors. In any event, the CAR1-CAR3 assay systems developed here provide the basis for identification of both direct acting ligand agonists of CAR as well as inverse agonists of the receptor in multiple mammalian species.

ETA, a triazole fungicide that has no registered uses, activated the CAR3 constructs from rat (up to 23-fold) and mouse (up to 16-fold) in a concentration-dependent manner at 10 and 30μM. The response with human CAR3 was only statistically significant at 30μM and represented only a 2.6-fold increase. No activation of dog CAR3 constructs was observed. ETA produced an increase in liver hepatocellular adenomas and/or carcinomas plus related non-neoplastic liver micropathology in long-term bioassays in both rats and mice, but it produced no effect on the liver in dogs after treatment for 3 or 6 months (Syngenta Crop Protection, LLC., personal communication). Therefore, the species differences in the CAR3 activation assays in mice, rats, and dogs correlated with the biological responses seen in the liver in prior *in vivo* bioassays. Further, while a possible indirect activation cannot be excluded, the large quantitative differences between rats/mice and humans for CAR3 activation may point to a species difference in the relative potency for CAR-mediated liver effects with ETA in humans compared with rodents. Thus, the assay systems developed here provide the basis for identification of qualitative or quantitative differences in species responses to direct CAR activation.

In summary, the results presented in this investigation demonstrate that the 5-aa insertion that typifies human CAR3 also lowers the constitutive activity and allows detection of ligand-activated receptor function in other species' CARs, while maintaining signature responses in each species to select

CAR ligands. These CAR variant constructs permit comparative evaluation of chemical effectors, including ligand activators and inverse agonists of CAR, across four mammalian species and provide a more sensitive approach to quantitative evaluation of species-specific differences in direct CAR activation. Coupled with *in vivo* assays in wild-type and humanized CAR mouse models (Ross *et al*., 2010), the CAR studies described here should permit further discrimination of the biological modes of action contributed by CAR in both normal physiology and in disease processes such as hepatocarcinogenesis.

SUPPLEMENTARY DATA

Supplementary data are available online at http://toxsci.oxfordjournals.org/.

FUNDING

National Institute of General Medical Sciences (GM066411 to C.J.O.); Syngenta Crop Protection, LLC., (task # 2227-09 to C.J.O.).

ACKNOWLEDGMENTS

The authors are indebted to Dr Stephen C. Strom (University of Pittsburgh) for his valuable assistance with provision of primary human hepatocyte samples and to Dr Joshua G. DeKeyser for his bioinfomatics insight. The authors also acknowledge the support and encouragement of Dr Gary Skiles (Amgen, Inc.) in the initial phase of these studies. A preliminary version of this investigation was presented at the 15th North American Regional ISSX Meeting, 2008, Abstract #12342, (Kari M. Morrissey, Gary L. Skiles, Adrian J. Fretland, Curtis J. Omiecinski, and Catherine L. Booth-Genthe).

REFERENCES

Arnold, K. A., Eichelbaum, M., and Burk, O. (2004). Alternative splicing affects the function and tissue-specific expression of the human constitutive androstane receptor. *Nucl. Recept.* **2,** 1.

Auerbach, S. S., Dekeyser, J. G., Stoner, M. A., and Omiecinski, C. J. (2007). CAR2 displays unique ligand binding and RXRalpha heterodimerization characteristics. *Drug Metab. Dispos.* **35,** 428–439.

Auerbach, S. S., Ramsden, R., Stoner, M. A., Verlinde, C., Hassett, C., and Omiecinski, C. J. (2003). Alternatively spliced isoforms of the human constitutive androstane receptor. *Nucleic Acids Res.* **31,** 3194–3207.

Auerbach, S. S., Stoner, M. A., Su, S., and Omiecinski, C. J. (2005). Retinoid X receptor-{alpha}-dependent transactivation by a naturally occurring structural variant of human constitutive androstane receptor (NR1I3). *Mol. Pharmacol.* **68,** 1239–1253.

Bruning, J. B., Parent, A. A., Gil, G., Zhao, M., Nowak, J., Pace, M. C., Smith, C. L., Afonine, P. V., Adams, P. D., Katzenellenbogen, J. A., *et al.* (2010). Coupling of receptor conformation and ligand orientation determine graded activity. *Nat. Chem. Biol.* **6,** 837–843.

Burk, O., Arnold, K. A., Nussler, A. K., Schaeffeler, E., Efimova, E., Avery, B. A., Avery, M. A., Fromm, M. F., and Eichelbaum, M. (2005). Antimalarial artemisinin drugs induce cytochrome P450 and MDR1 expression by activation of xenosensors pregnane X receptor and constitutive androstane receptor. *Mol. Pharmacol.* **67,** 1954–1965.

Chang, T. K., and Waxman, D. J. (2006). Synthetic drugs and natural products as modulators of constitutive androstane receptor (CAR) and pregnane X receptor (PXR). *Drug Metab. Rev.* **38,** 51–73.

Chen, T., Tompkins, L. M., Li, L., Li, H., Kim, G., Zheng, Y., and Wang, H. (2010). A single amino acid controls the functional switch of human constitutive androstane receptor (CAR) 1 to the xenobiotic-sensitive splicing variant CAR3. *J. Pharmacol. Exp. Ther.* **332,** 106–115.

Dekeyser, J. G., Laurenzana, E. M., Peterson, E. C., Chen, T., and Omiecinski, C. J. (2011). Selective phthalate activation of naturally occurring human constitutive androstane receptor splice variants and the pregnane x receptor. *Toxicol. Sci.* **120,** 381–391.

Dekeyser, J. G., and Omiecinski, C. J. (2010). Constitutive androstane receptor. In *Comprehensive Toxicology: Vol. 2-Cellular and Molecular Toxicology*, 2nd ed., (C.A. McQueen, Ed.), pp. 169–181. Elsevier, New York, NY.

Dekeyser, J. G., Stagliano, M. C., Auerbach, S. S., Prabu, K. S., Jones, A. D., and Omiecinski, C. J. (2009). Di(2-ethylhexyl) phthalate is a highly potent agonist for the human constitutive androstane receptor splice variant, CAR2. *Mol. Pharmacol.* **75,** 1005–1013.

Dussault, I., Lin, M., Hollister, K., Fan, M., Termini, J., Sherman, M. A., and Forman, B. M. (2002). A structural model of the constitutive androstane receptor defines novel interactions that mediate ligand-independent activity. *Mol. Cell. Biol.* **22,** 5270–5280.

Echchgadda, I., Song, C. S., Oh, T., Ahmed, M., and De La Cruz, I. J., Chatterjee, B. 2007 The xenobiotic-sensing nuclear receptors pregnane X receptor, constitutive androstane receptor, and orphan nuclear receptor hepatocyte nuclear factor 4alpha in the regulation of human steroid-/bile acid-sulfotransferase. *Mol. Endocrinol.* **21,** 2099–2111.

Faucette, S. R., Zhang, T. C., Moore, R., Sueyoshi, T., Omiecinski, C. J., LeCluyse, E. L., Negishi, M., and Wang, H. (2007). Relative activation of human pregnane X receptor versus constitutive androstane receptor defines distinct classes of CYP2B6 and CYP3A4 inducers. *J. Pharmacol. Exp. Ther.* **320**(1), 72–80.

Forman, B. M., Tzameli, I., Choi, H. S., Chen, J., Simha, D., Seol, W., Evans, R. M., and Moore, D. D. (1998). Androstane metabolites bind to and deactivate the nuclear receptor CAR- beta. *Nature* **395,** 612–615.

Gao, J., and Xie, W. (2010). PXR and CAR at the crossroad of drug metabolism and energy metabolism. *Drug Metab. Dispos.* **38,** 2091–2095.

Gonzalez, F. C. M. M., Oinonen, C., Dunlop, T. W., and Carlberg, C. (2003). Characterization of DNA complexes formed by the nuclear receptor constitutive androstane receptor. *J. Biol. Chem.* **278,** 43299–43310.

Guex, N., and Peitsch, M. C. (1997). SWISS-MODEL and the Swiss-PdbViewer: an environment for comparative protein modeling. *Electrophoresis* **18,** 2714–2723.

Holsapple, M. P., Pitot, H. C., Cohen, S. M., Boobis, A. R., Klaunig, J. E., Pastoor, T., Dellarco, V. L., and Dragan, Y. P. (2006). Mode of action in relevance of rodent liver tumors to human cancer risk. *Toxicol. Sci.* **89**(1), 51–56.

Huang, W., Zhang, J., and Moore, D. D. (2004a). A traditional herbal medicine enhances bilirubin clearance by activating the nuclear receptor CAR. *J. Clin. Invest.* **113,** 137–143.

Huang, W., Zhang, J., Washington, M., Liu, J., Parant, J. M., Lozano, G., and Moore, D. D. (2005). Xenobiotic stress induces hepatomegaly and liver

tumors via the nuclear receptor constitutive androstane receptor. *Mol. Endocrinol.* **19,** 1646–1653.

Huang, W., Zhang, J., Wei, P., Schrader, W. T., and Moore, D. D. (2004b). Meclizine is an agonist ligand for mouse constitutive androstane receptor (CAR) and an inverse agonist for human CAR. *Mol. Endocrinol.* **18,** 2402–2408.

Jinno, H., Tanaka-Kagawa, T., Hanioka, N., Ishida, S., Saeki, M., Soyama, A., Itoda, M., Nishimura, T., Saito, Y., Ozawa, S., *et al.* (2004). Identification of novel alternative splice variants of human constitutive androstane receptor and characterization of their expression in the liver. *Mol. Pharmacol.* **65,** 496–502.

Kobayashi, K., Yamanaka, Y., Iwazaki, N., Nakajo, I., Hosokawa, M., Negishi, M., and Chiba, K. (2005). Identification of HMG-CoA reductase inhibitors as activators for human, mouse and rat constitutive androstane receptor. *Drug Metab. Dispos.* **33,** 924–929.

Kozak, M. (1987). An analysis of 5'-noncoding sequences from 699 vertebrate messenger RNAs. *Nucleic Acids Res.* **15,** 8125–8148.

Lamba, J., Lamba, V., and Schuetz, E. (2005). Genetic variants of PXR (NR1I2) and CAR (NR1I3) and their implications in drug metabolism and pharmacogenetics. *Curr. Drug Metab.* **6,** 369–383.

Lamminpaa, A., Pukkala, E., Teppo, L., and Neuvonen, P. J. (2002). Cancer incidence among patients using antiepileptic drugs: a long-term follow-up of 28,000 patients. *Eur. J. Clin. Pharmacol.* **58,** 137–141.

Laurie, A. T., and Jackson, R. M. (2005). Q-SiteFinder: an energy-based method for the prediction of protein-ligand binding sites. *Bioinformatics* **21,** 1908–1916.

Livak, K. J., and Schmittgen, T. D. (2001). Analysis of relative gene expression data using real-time quantitative PCR and the 2(-Delta Delta C(T)) Method. *Methods* **25,** 402–408.

Maglich, J. M., Lobe, D. C., and Moore, J. T. (2009). The nuclear receptor CAR (NR1I3) regulates serum triglyceride levels under conditions of metabolic stress. *J. Lipid Res.* **50,** 439–445.

Maglich, J. M., Parks, D. J., Moore, L. B., Collins, J. L., Goodwin, B., Billin, A. N., Stoltz, C. A., Kliewer, S. A., Lambert, M. H., Willson, T. M., *et al.* (2003). Identification of a novel human constitutive androstane receptor (CAR) agonist and its use in the identification of CAR target genes. *J. Biol. Chem.* **278,** 17277–17283.

Maglich, J. M., Watson, J., McMillen, P. J., Goodwin, B., Willson, T. M., and Moore, J. T. (2004). The nuclear receptor CAR is a regulator of thyroid hormone metabolism during caloric restriction. *J. Biol. Chem.* **279,** 19832–19838.

Moore, J. T., Moore, L. B., Maglich, J. M., and Kliewer, S. A. (2003). Functional and structural comparison of PXR and CAR. *Biochim. Biophys. Acta* **1619,** 235–238.

Moore, L. B., Parks, D. J., Jones, S. A., Bledsoe, R. K., Consler, T. G., Stimmel, J. B., Goodwin, B., Liddle, C., Blanchard, S. G., Willson, T. M., *et al.* (2000). Orphan nuclear receptors constitutive androstane receptor and pregnane X receptor share xenobiotic and steroid ligands. *J. Biol. Chem.* **275,** 15122–15127.

Mutoh, S., Osabe, M., Inoue, K., Moore, R., Pedersen, L., Perera, L., Rebolloso, Y., Sueyoshi, T., and Negishi, M. (2009). Dephosphorylation of threonine 38 is required for nuclear translocation and activation of human xenobiotic receptor CAR (NR1I3). *J. Biol. Chem.* **284,** 34785–34792.

Page, J. L., Johnson, M. C., Olsavsky, K. M., Strom, S. C., Zarbl, H., and Omiecinski, C. J. (2007). Gene expression profiling of extracellular matrix as an effector of human hepatocyte phenotype in primary cell culture. *Toxicol. Sci.* **97,** 384–397.

Pascussi, J. M., Gerbal-Chaloin, S., Duret, C., Daujat-Chavanieu, M., Vilarem, M. J., and Maurel, P. (2008). The tangle of nuclear receptors that controls xenobiotic metabolism and transport: crosstalk and consequences. *Annu. Rev. Pharmacol. Toxicol.* **48,** 1–32.

Reschly, E. J., and Krasowski, M. D. (2006). Evolution and function of the NR1I nuclear hormone receptor subfamily (VDR, PXR, and CAR) with respect to metabolism of xenobiotics and endogenous compounds. *Curr. Drug Metab.* **7,** 349–365.

Ross, J., Plummer, S. M., Rode, A., Scheer, N., Bower, C. C., Vogel, O., Henderson, C. J., Wolf, C. R., and Elcombe, C. R. (2010). Human constitutive androstane receptor (CAR) and pregnane X receptor (PXR) support the hypertrophic but not the hyperplastic response to the murine nongenotoxic hepatocarcinogens phenobarbital and chlordane in vivo. *Toxicol. Sci.* **116,** 452–466.

Scheer, N., Ross, J., Rode, A., Zevnik, B., Niehaves, S., Faust, N., and Wolf, C. R. (2008). A novel panel of mouse models to evaluate the role of human pregnane X receptor and constitutive androstane receptor in drug response. *J. Clin. Invest.* **118,** 3228–3239.

Shan, L., Vincent, J., Brunzelle, J. S., Dussault, I., Lin, M., Ianculescu, I., Sherman, M. A., Forman, B. M., and Fernandez, E. J. (2004). Structure of the murine constitutive androstane receptor complexed to androstenol: a molecular basis for inverse agonism. *Mol. Cell* **16,** 907–917.

Sidhu, J. S., Liu, F., and Omiecinski, C. J. (2004). Phenobarbital responsiveness as a uniquely sensitive indicator of hepatocyte differentiation status: requirement of dexamethasone and extracellular matrix in establishing the functional integrity of cultured primary rat hepatocytes. *Exp. Cell Res.* **292,** 252–264.

Song, J. C., and Deresinski, S. (2005). Hepatotoxicity of antifungal agents. *Curr. Opin. Investig. Drugs* **6,** 170–177.

Sueyoshi, T., and Negishi, M. (2001). Phenobarbital response elements of cytochrome p450 genes and nuclear receptors. *Annu. Rev. Pharmacol. Toxicol.* **41,** 123–143.

Suino, K., Peng, L., Reynolds, R., Li, Y., Cha, J. Y., Repa, J. J., Kliewer, S. A., and Xu, H. E. (2004). The nuclear xenobiotic receptor CAR: structural determinants of constitutive activation and heterodimerization. *Mol. Cell* **16,** 893–905.

Tzameli, I., Pissios, P., Schuetz, E. G., and Moore, D. D. (2000). The xenobiotic compound 1,4-bis[2-(3,5-dichloropyridyloxy)]benzene is an agonist ligand for the nuclear receptor CAR. *Mol. Cell. Biol.* **20,** 2951–2958.

Wang, H., Faucette, S., Sueyoshi, T., Moore, R., Ferguson, S., Negishi, M., and LeCluyse, E. L. (2003). A novel distal enhancer module regulated by pregnane X receptor/constitutive androstane receptor is essential for the maximal induction of CYP2B6 gene expression. *J. Biol. Chem.* **278,** 14146–14152.

Whysner, J., Ross, P. M., and Williams, G. M. (1996). Phenobarbital mechanistic data and risk assessment: enzyme induction, enhanced cell proliferation, and tumor promotion. *Pharmacol. Ther.* **71**(1-2), 153–191.

Xu, R. X., Lambert, M. H., Wisely, B. B., Warren, E. N., Weinert, E. E., Waitt, G. M., Williams, J. D., Collins, J. L., Moore, L. B., Willson, T. M., *et al.* (2004). A structural basis for constitutive activity in the human CAR/RXRalpha heterodimer. *Mol. Cell* **16,** 919–928.

Yamamoto, Y., Moore, R., Goldsworthy, T. L., Negishi, M., and Maronpot, R. R. (2004). The orphan nuclear receptor constitutive active/androstane receptor is essential for liver tumor promotion by phenobarbital in mice. *Cancer Res.* **64,** 7197–7200.

Yoshikado, T., Takada, T., Yamamoto, T., Yamaji, H., Ito, K., Santa, T., Yokota, H., Yatomi, Y., Yoshida, H., Goto, J., *et al.* (2011). Itraconazole-induced cholestasis: involvement of the inhibition of bile canalicular phospholipid translocator MDR3/ABCB4. *Mol. Pharmacol.* **79,** 241–250.